# Early stage seismic damage assessment of reinforced concrete walls considering crack conditions


**S. Kono**
*Materials and Structures Laboratory, Tokyo Institute of Technology, Japan*

**J. Yoshimura, M. Sakashita, M. Nishiyama**
*Dept. of Architecture and Architectural Engineering, Kyoto University, Japan*

**T. Nagae, T. Matsumori**
*National Research Institute for Earth Science and Disaster Prevention, Japan*

**T. Mukai, M. Tani and H. Fukuyama**
*Building Research Institute, Japan*

**I. Amano**
*Hozen Kogaku Kenkyusho, Japan*

**SUMMARY:**
Two 40% scale rectangular section wall specimens with different amount of confining reinforcement were tested to study the damage process under static cyclic loading. Crack width was recorded with electronic crack gages and crack condition was quantified at different load levels in terms of number and width of cracks in order to study the correlation between crack condition and damage level. Based on the experimental results, an existing numerical model to predict crack condition was evaluated. Then static test results were compared to crack conditions observed for structural walls of 2010 real-scale four-story reinforced concrete buildings dynamically tested on the E-Defense shaking table in Japan.

*Keywords: Damage assessment, Crack evaluation, RC structural walls, real scale dynamic test*

## 1. INTRODUCTION

Performance based design criteria have been slowly spreading for reinforced concrete structures since large-scale earthquakes, such as the 1994 Northridge EQ and the 1995 Kobe EQ, hit major urban cities in 1990s. Researchers made efforts to determine characteristic points such as cracking, yielding, peak, and ultimate points and it has been becoming possible to predict these points with good accuracy. Based on these characteristic points, performance criteria may be determined for different limit states; serviceability, reparability, safety and collapse prevention limit states. However, it is still difficult to accurately simulate damage level which determines retrofit schemes and cost. For concrete members, number, width and length of cracks are important factors to determine early stage seismic damage. However, quantification of cracks is not easy especially for two dimensional members like structural walls since a large amount of meandering cracks emerge. It is even more difficult to utilize crack conditions to describe the damage level.

Two 40% scale structural wall specimens were tested statically by varying amount of confining reinforcement to study the seismic performance under static cyclic loading. Damage states at different loading stages were recorded with displacement gages and high resolution digital cameras. Number and width of cracks were quantified at different load levels. Based on the experimental results, an existing numerical model to predict crack conditions was used to simulate the test results. Then, static test results were compared to crack conditions observed for structural walls of the 2010 real scale four-story reinforced concrete building dynamically tested on the E-Defense shaking table.

## 2. STATICALLY TESTED SPECIMENS

Main results of static test are explained but the minimum information on test setup is presented since the companion paper (Kono et al. 2012) describes full detail of the experiment.

### 2.1. Test setup

Two 40% scale specimens are prepared by changing the amount of shear reinforcement as shown in **Figure 1**. Specimens NC40 and NC80 had same section dimensions with different amount of confinement. Table 1 lists major test variables. The shear capacity was set more than 1.25 times larger than the flexural capacity so that they failed in flexure mode. **Table 2** and **Table 3** list the mechanical properties of concrete and reinforcement. The lateral load was applied at the center of the top loading beam, which is 3000 mm high from the top of the foundation. Hence, the shear span ratio was 1.71. The axial load of 1500 kN was applied constantly by two hydraulic jacks to keep the axial load level of 0.20 for confined region, that is, 0.11 for the total area of the section.

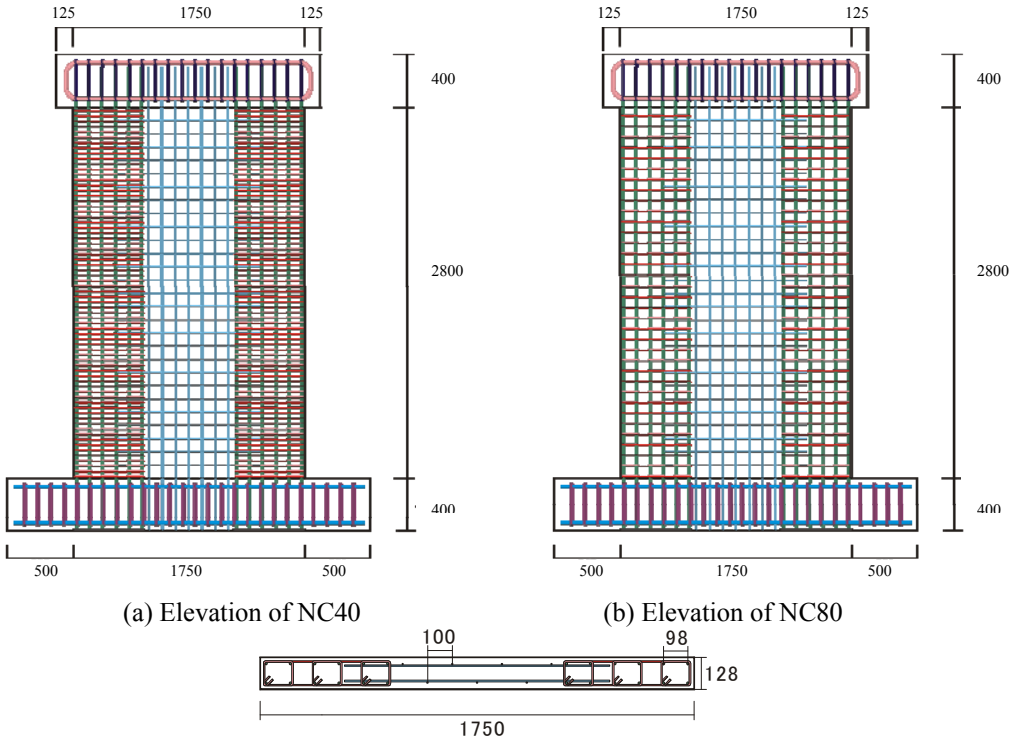


**Figure 1.** Dimensions and reinforcement arrangement (Unit: mm)

**Table 1.** Test variables

| Specimen | Width & height of wall panel (mm) | Confined area | | | Wall panel | |
|---|---|---|---|---|---|---|
| | | Section dimension (mm) | Longitudinal reinforcement (rebar ratio) | Shear reinforcement (rebar ratio) | Thickness (mm) | Shear reinforcement (rebar ratio) |
| NC40 | 1750 x 2800 | 128x520 | 12-D10 (1.29%) | 4-D6@40 (2.47%) | 128 | D6@100 Staggered (0.25%) |
| NC80 | | | | 4-D6@80 (1.24%) | | |

**Table 2.** Mechanical properties of concrete

| Specimen | Compressive strength (MPa) | Young's modulus (GPa) | Splitting strength (MPa) |
|---|---|---|---|
| NC40, NC80 | 52.5 | 30.1 | 3.66 |

**Table 3.** Mechanical properties of reinforcement

| Bar type | Yield strength (MPa) | Young's modulus (GPa) | Tensile strength (MPa) |
|---|---|---|---|
| D6 | 387 | 189 | 496 |
| D10 | 377 | 194 | 533 |

### 2.2. Test results

**Figure 2** shows lateral load - drift angle relations. Drift was measured at the center of the top loading beam. Both specimens yielded in flexure, reached the peak point, and deformed until the failure with minor degradation of lateral load carrying capacity. The ultimate failure was caused by the crushing of confined concrete. It is interesting that the hysteresis curves had very small residual drift at most cycles. It is probably due to high concrete strength and axial load level which made specimens behave like post-tensioned precast concrete structures. Discussion on this issue will be made elsewhere. The figures show the characteristic points (cracking, yielding, peak load, and ultimate deformation) by different marks. The ultimate deformation is defined by 20% degradation of load carrying capacity from the peak.

**Figure 3** shows crack patterns after three different drift angles. Red and blue lines represent cracks in positive and negative directions, respectively. NC40 and NC80 have flexure-shear cracks and it is interesting that some shear cracks extend to flexural cracks although the opposite process normally takes place. At the final stage, the failure was brittle since core concrete crushed and lateral load dropped. Crushing of concrete extended to the center of the wall panel and wall panels finally buckled at the compression region.

Crack width was measured in two ways. One method employed electronic crack gages and the other employed a digital camera. When a crack crossed the center line of the wall, an electronic crack gage (Tokyo Sokki, PI2) was attached on the intersection of the crack and center line. The data is continuously recorded afterward with other electronic measuring devices. The obtained crack width data was shifted so that the minimum value at the cracked cycle became zero. The other device is a high resolution digital camera (Canon Eos 5, Mark II). Digital photo was processed with a crack analysing software (HMME, 2012) to obtain location, width and length of cracks. Although the software is powerful, it was used to obtain the crack width at the center line this time. The total residual crack width, $\Sigma_r W_{cr}$, obtained with two methods is shown in terms of the shear component of residual drift angle, ${}_rR_s$, in **Figure 4**(a). It is noted that the measurement was conducted for the area lower than 1500 mm due to the difficult accessibility to the higher region of the specimen. Since the diagonal cracks along the center line exist only below 1500 mm, the measuring procedure is considered reasonable. Photo values are larger than gage values for both specimens. It is interesting that the relation between $\Sigma_r W_{cr}$ and ${}_rR_s$ is somehow linear.

Based on the linear relation in **Figure 4**(a), the assumption is made on the shear deformation as shown in **Figure 5**. The figure assumes that the shear deformation is totally due to shear cracks. Hence, the shear drift angle, $R_s$, is expressed as the horizontal component of total crack width at any loading stage. It is expressed as follows.

$$R_s = \frac{\left(\sum W_{cr}\right)\cos\theta}{H} \quad \textbf{(1)}$$

where $\Sigma W_{cr}$ is the summation of all crack widths, $\theta$ is the angle of cracks, $H$ is the wall height, and all quantities are shown in **Figure 5**. The solid line with arrow mark in **Figure 4**(a) represents **Eq. (1)** for both NC40 and NC80. It is seen that gage values are somehow close to **Eq. (1)**.

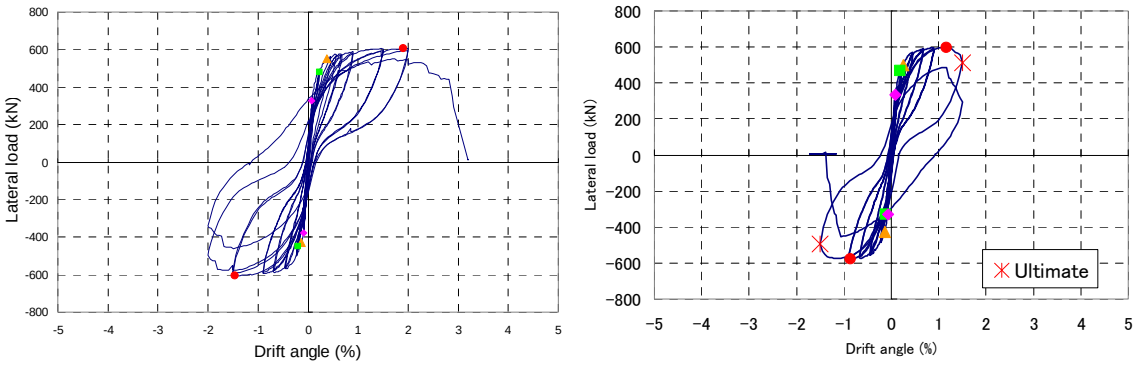


(a) NC40 (b) NC80

**Figure 2.** Lateral load - drift angle relation

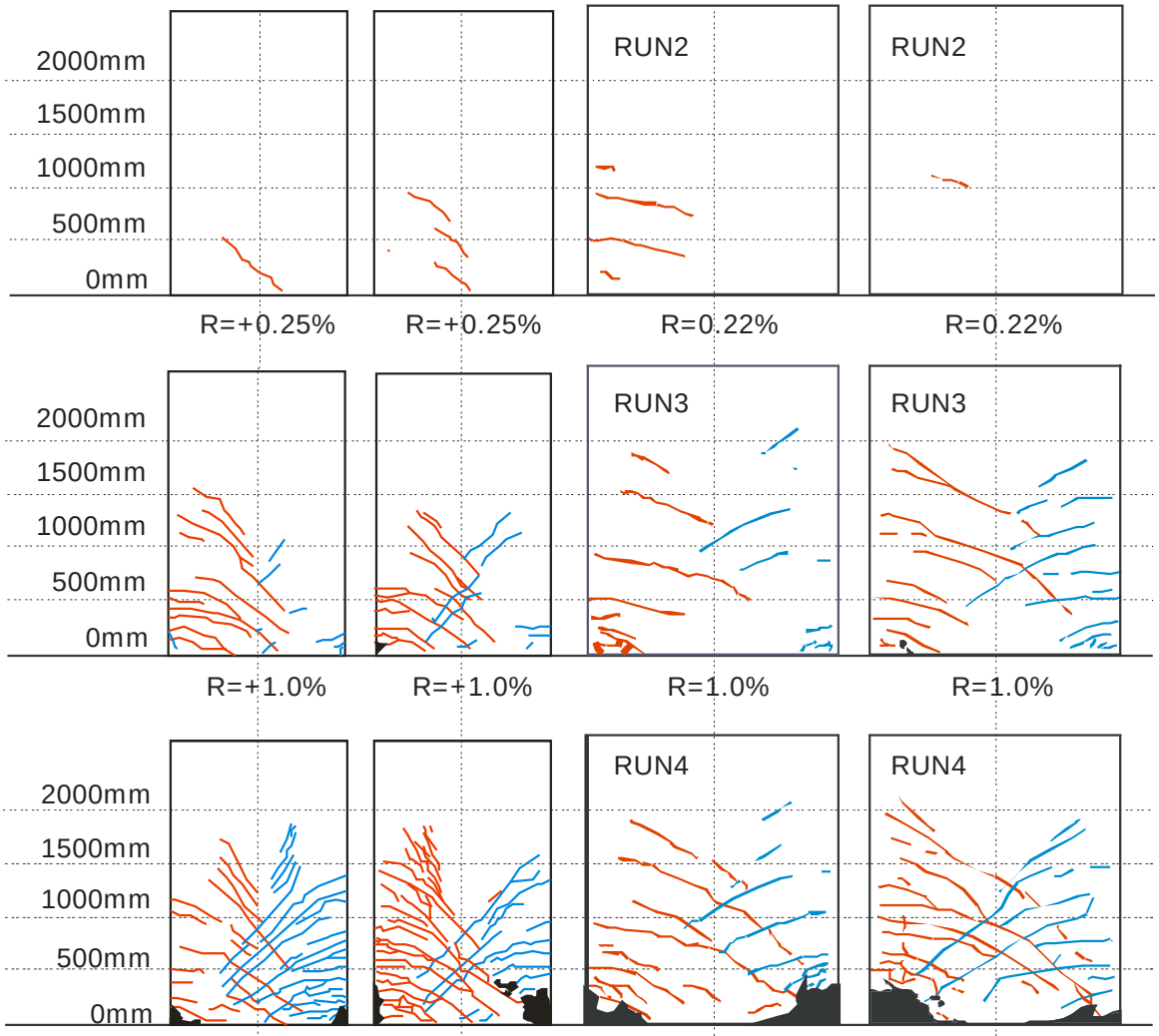


(a) NC40 (b) NC80 (c) Wall A d) Wall C

**Figure 3.** Crack patterns at end of selected cycles (R represents the maximum experienced drift)

Based on Eq. (1), the total residual crack width, $\Sigma_r W_{cr}$, was computed using the residual shear drift obtained experimentally. The computed results are compared to gage and photo widths in **Figure 6**(a) and (b) which show total residual crack width ($\Sigma_r W_{cr}$) and cycle peak shear drift ($_pR_s$) relations. The computed results agree well with gage width.

Next, the average residual crack width, $_rW_{cr\text{-}av}$, is obtained by dividing the total residual crack width ($\Sigma_r W_{cr}$) by the number of cracks. The number of cracks ($_cN$) was obtained from the spacing of cracks. The vertical spacing of cracks, $_cL$, is based on **Eq. (2)** which is empirical and proposed in the AIJ guidelines (AIJ, 2004).

$$_cL = \frac{3 f_t t_w [2.6 - 0.93 \log\{0.5(S_x + S_y)\}]}{n \tau_{\max} (\phi_x + \phi_y) \sin\theta} \cdot \frac{1}{2} \left( \frac{S_x}{\cos\theta} + \frac{S_y}{\sin\theta} \right) \quad \textbf{(2)}$$

where $f_t$ is the tensile strength of concrete, $t_w$ is the wall thickness, $S_x$ and $S_y$ are spacings of horizontal and vertical wall reinforcement, $\phi_x$ and $\phi_y$ are diameters of horizontal and vertical wall reinforcement, $n$ is the layer of reinforcement, $\tau_{max}$ is the bond strength of reinforcement and $\theta$ is the angle of cracks defined in **Figure 5**. Once the spacing of cracks ($_cL$) is known, the number of cracks ($_cN$) can be obtained by dividing the wall height ($H$) by the spacing of cracks ($_cL$). However, as can be seen from **Figure 3**, shear cracks stayed only at the lower portion of the wall and never occurred at higher portion. Hence, instead of the wall height ($H$=*3000mm*), experimentally measured height of cracked region ($H'$) was used for the vertical length of cracked region. Then $_cN$ may be obtained as $_cN = H'/_cL$. The computed and experimental vertical spacing of cracks, $_cL$ and $_eL$, and the number of cracks, $_cN$ and $_eL$, are compared in **Table 4**. **Equation (2)** gives good agreement at peak drift of 0.5% - 1.5% for NC40 and 0.25% for NC80. Disagreement at other drift was caused because the equation gives only one number for a specimen and does not reflect the fact that the number of cracks increases gradually as the specimens deform.

Using the total residual crack width ($\Sigma_r W_{cr}$) and the number of cracks ($_cN$), the relation between average residual crack width ($_rW_{cr\text{-}av}$) and cycle peak shear drift ($_pR_s$) was obtained as shown in **Figure 7**. Although the error is not necessarily small, the computed results somehow represent gage and photo widths.

**Table 4.** Comparison between experimental and computed crack spacing and number

| Specimen | $_pR$ (%) | $_rR_s$ (%) | Crack spacing | | Number of cracks | | | $_rW_{cr\text{-}ave}$ (mm) |
|---|---|---|---|---|---|---|---|---|
| | | | $_eL$ (mm) | $_cL$ (mm) | $_eN$ | $_cN$ | $_eN/_cN$ | |
| NC40 | 0.25 | 0.010 | 0 | 347 | 1 | 1.0 | 1.00 | 0.07 |
| | 0.50 | 0.024 | 399 | | 3 | 3.3 | 0.91 | 0.07 |
| | 0.75 | 0.021 | 399 | | 3 | 3.3 | 0.91 | 0.12 |
| | 1.00 | 0.035 | 399 | | 3 | 3.3 | 0.91 | 0.14 |
| | 1.50 | 0.050 | 399 | | 3 | 3.3 | 0.91 | 0.21 |
| | 2.00 | 0.042 | 234 | | 6 | 4.4 | 1.37 | 0.24 |
| NC80 | 0.25 | 0.000 | 344 | 347 | 2 | 2.0 | 1.00 | 0.06 |
| | 0.50 | -0.002 | 219 | | 3 | 2.3 | 1.33 | 0.13 |
| | 0.75 | 0.009 | 206 | | 5 | 3.4 | 1.48 | 0.10 |
| | 1.00 | 0.015 | 206 | | 5 | 3.4 | 1.48 | 0.15 |
| | 1.50 | 0.205 | 165 | | 6 | 3.4 | 1.78 | 1.27 |
| Wall A | 0.22*1 | 0.00 | NA | 253 | 0 | 1.0 | 0.00 | 0.00 |
| | 1.0*2 | 0.04 | NA | | 1 | 1.0 | 1.00 | 0.01 |
| | 3.4*3 | 0.34 | 432 | | 2 | 2.7 | 0.74 | 0.02 |
| Wall C | 0.22*1 | 0.00 | NA | 221 | 0 | 1.0 | 0.00 | 0.00 |
| | 1.0*2 | 0.04 | NA | | 1 | 1.0 | 1.00 | 0.09 |
| | 3.4*3 | 0.34 | 389 | | 3 | 4.5 | 0.66 | 0.29 |

*1, *2, *3 correspond to Run 2, 3 and 4, respectively.
Subscripts '*e*' and '*c*' represent experimental and computed values, respectively.

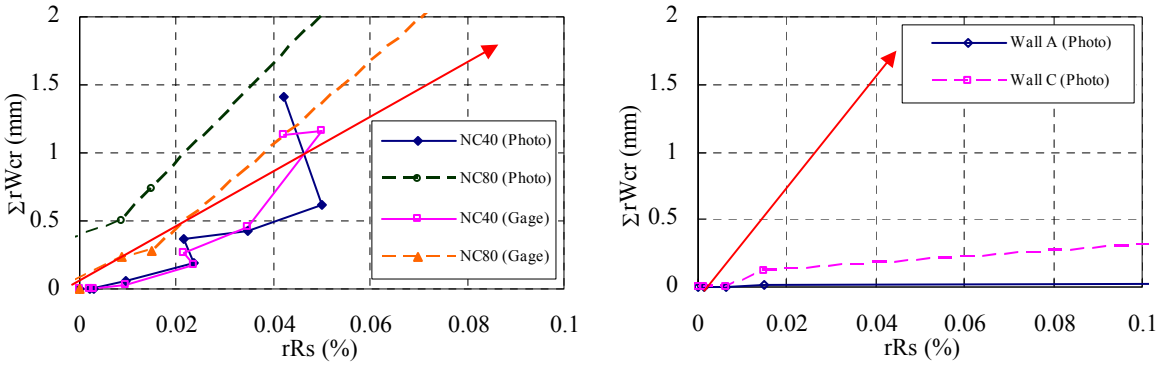


(a) NC40 and NC80 (b) Walls A and C

**Figure 4.** Relations between total residual shear crack width ( $\Sigma_r W_{cr}$) and residual shear drift angle ($_rR_s$)

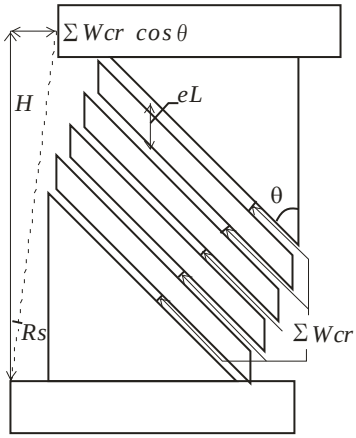


**Figure 5.** Idealized concept of shear deformation and shear crack distribution

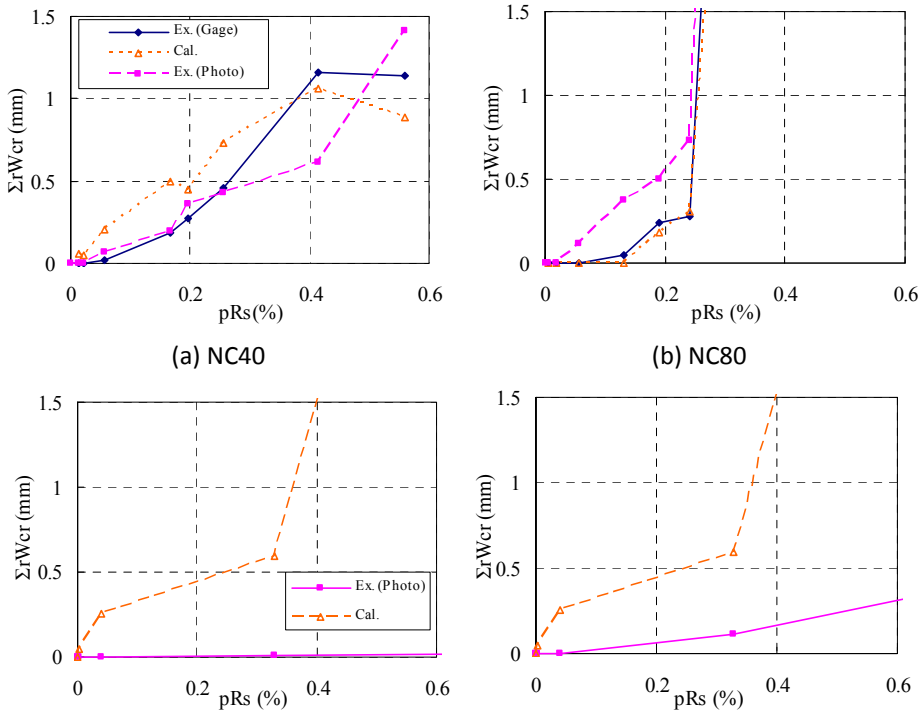


(a) NC40 (b) NC80

(c) Wall A (d) Wall C

**Figure 6.** Total residual shear crack width ( $\Sigma_r W_{cr}$) - cycle peak shear drift ($_pR_s$) relations

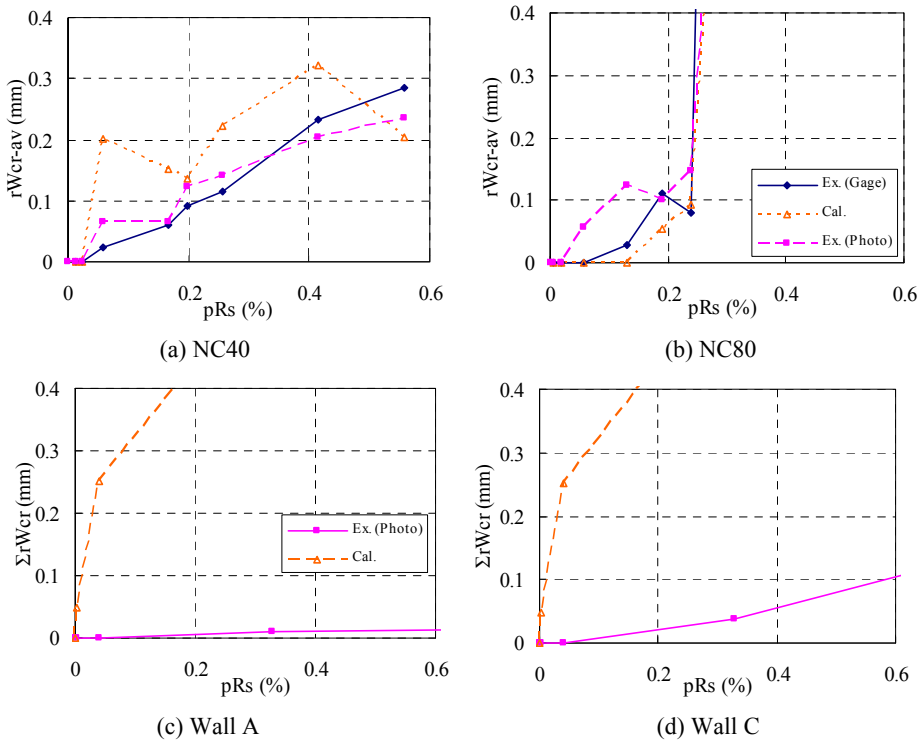


(a) NC40 (b) NC80

(c) Wall A (d) Wall C

**Figure 7.** Mean residual shear crack width ($_rW_{cr\text{-}av}$) - cycle peak shear drift ($_pR_s$) relations

## 3. DYNAMICALLY TESTED REAL SCALE SPECIMEN

A full-scale, four-story RC building specimen tested on the E-Defense shake table (Nagae et al. 2011a, 2011b, 2012). The building utilized a conventional reinforced concrete (RC) structural system with shear walls in transverse direction and moment frames in longitudinal direction.

### 3.1. Test setup

Slightly different detailing has been provided within the yielding regions (plastic hinge regions) of the shear walls on the north and south sides of the RC building to investigate the role of detailing on damageability, lateral strength degradation, and, potentially, the loss of axial load carrying capacity.

Dimensions and reinforcement of the building specimen is shown in **Figure 8**. Cross-section dimensions of columns were 500 mm × 500 mm, and walls were 250 mm ×2500 mm. A 130 mm-thick floor slab was used at floor levels 2 through 4 and at the roof level. Detailed information on member geometry and reinforcement used is given in the reference (Nagae et al. 2011b). The concrete compressive strength was 39.6 MPa and SD345 D19 (fy=380 MPa) and D22 (fy=370 MPa) bars were used for primary longitudinal reinforcement.

### 3.2. Damage after each Runs 2, 3 and 4

**Table 6** lists the maximum story drift at the first floor and this paper describes Runs 2, 3 and 4. **Figure 9** shows story shear - story drift angle relations for Run 2, 3 and 4. Run 2 is in a linear elastic range, Run 3 exceeded cracking but did not reach yielding range, Run 4 exceeded yielding range. Damage was recorded after each run as shown in **Figure 3**. Wall C, which had lesser reinforcement, caused larger number of cracks than Wall A. For Runs 2 and 3, the damage condition for static test at comparable drift is placed on the side. The number of cracks is less for dynamic test. At Run 4, the maximum drift was 3.4% and much larger than the static test placed on the side but Walls A and C had less number of cracks. The number and spacing of cracks for Walls A and C are listed with NC40 and

NC80 in **Table 4**.

Photos taken with a digital camera (Canon Eos 5, Mark II) was used to measure cracks with the same crack analysing software. To compare the results with static test, the crack width was measured at the center line of the wall at the first floor and shown in **Figure 4**(b). Different from the static test, Walls A and C show much smaller crack width than the red arrow line. It is probably because Walls A and C slided at the base and wall deformation is smaller than expected.

Data was similarly treated with NC40 and NC80 to obtain **Figure 6** and **Figure 7**. Since the crack width was not picked up properly, the prediction is much larger than the test results. Walls A and C shows that the existing crack evaluation procedure by AIJ guidelines need some special care to measure shear drift angle. If the drift had been measured by excluding the slip, the simulation would be much better.

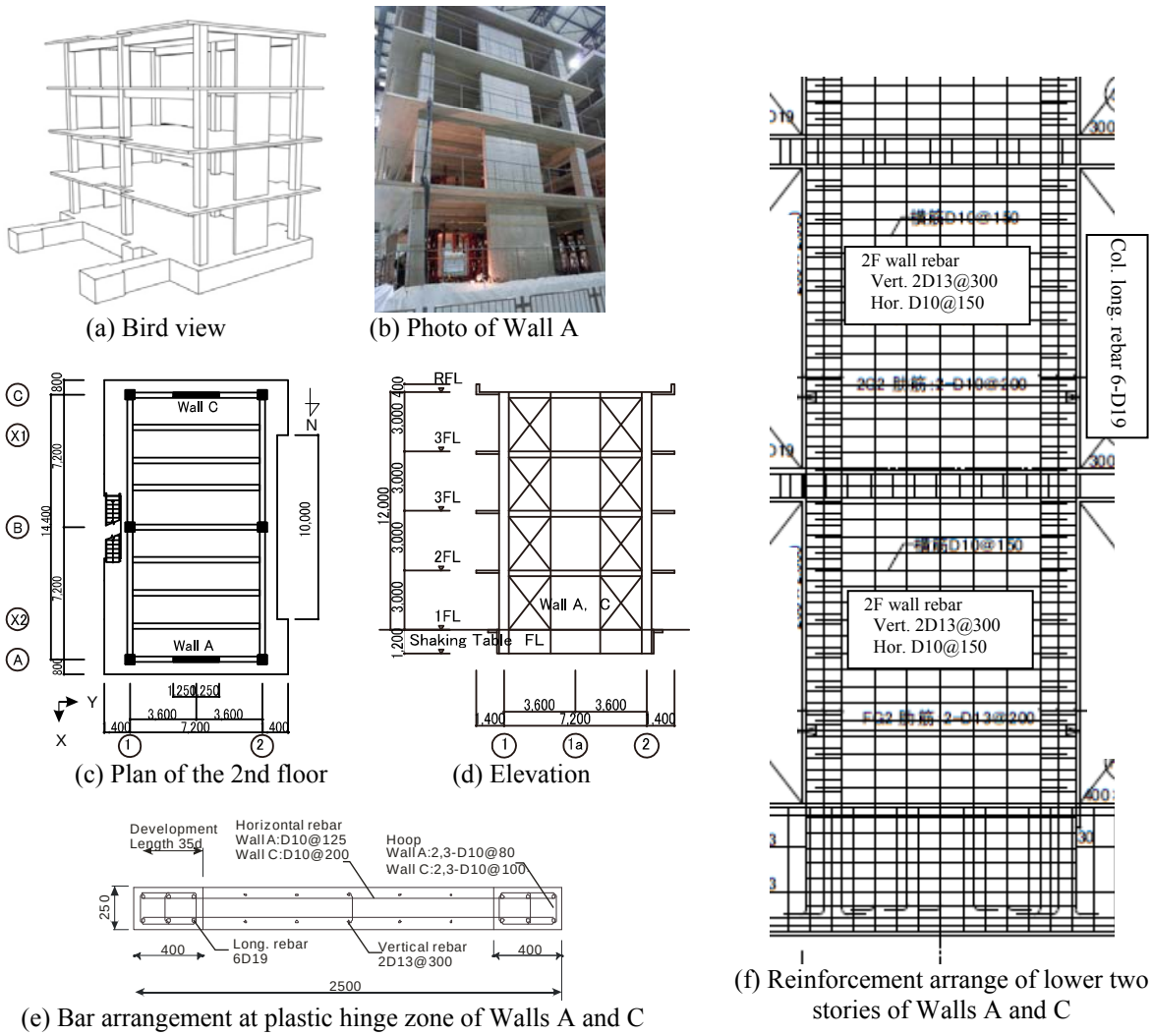


**Figure 8.** Walls of real scale RC building specimen tested at E-Defense in Japan

**Table 5.** Dimensions and reinforcement of Walls A and C.

| Name | Wall Size at each story (mm) | Confined area (250 x 400 mm) | | Wall (t=250mm) | |
|---|---|---|---|---|---|
| | | Long. Rebar | Shear rebar | Vert. rebar | Hor. Rebar |
| Wall A | t=250 w=2500 H=2400 | 6-D19 | 2,3-D10@80 | 2D13@300 | 2D10@125 |
| Wall C | | | 2,3-D10@100 | | 2D10@200 |

**Table 6.** Excitation program and the maximum story drift at the first floor

| RUN | Input ground motion | Maximum story drift (%) | |
|---|---|---|---|
| | | X | Y |
| 1 | JMA-Kobe-10% | 0.05 | 0.06 |
| 2 | JMA-Kobe-25% | 0.2 | 0.3 |
| 3 | JMA-Kobe-50% | 1.6 | 1.0 |
| 4 | JMA-Kobe-100% | 3.4 | 3.4 |
| 5 | JR-Takatori-40% | 3.4 | 2.7 |
| 6 | JR-Takatori-60% | 4.6 | 5.1 |

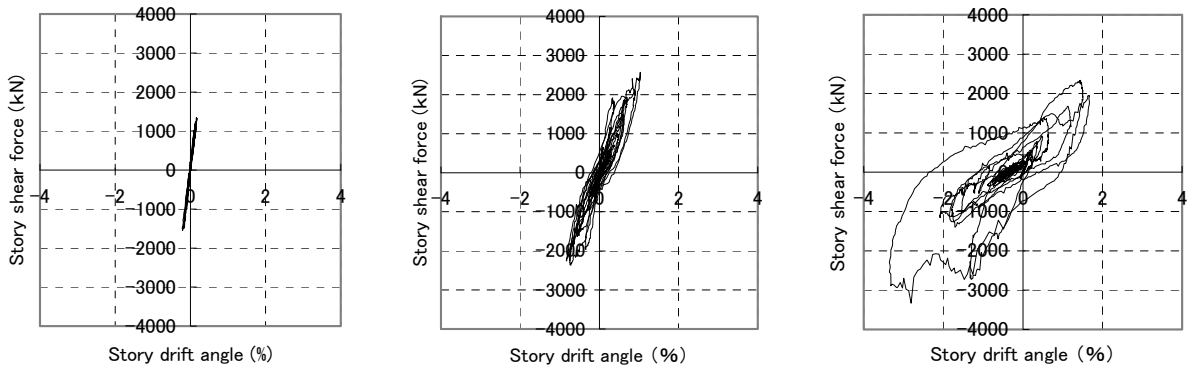


(a) Run 2 (b) Run 3 (c) Run 4

**Figure 9.** Story shear - story drift angle relations in wall direction

## 4. CONCLUSIONS

Structural walls tested statically and dynamically are introduced to compare the damage conditions.

- Statically tested walls had larger number of cracks than dynamically tested walls.
- Crack gages successfully measure crack opening continuously. Digital photo images with crack analysing software is a power tool to evaluate the overall crack properties and they evaluated crack width with similar precision to crack gages for statically tested specimens. However, they did not provide expected crack width for dynamically tested specimens probably due to the sliding at the wall base.
- Although some experimental results ($_rR_s$, $H'$) were used, the current AIJ guidelines is able to simulate the total and mean residual shear crack widths, the spacing of cracks with some extent of accuracy. Hence, it is concluded that it is a reasonable assumption that the shear deformation is totally based on the crack width for the sake of evaluating shear crack conditions.

**AKCNOWLEDGEMENT**
The static test was financially supported by the Japanese Ministry of Land, Infrastructure, Transportation and Tourism. The dynamic test was conducted by National Research Institute for Earth Science and Disaster

Prevention (NIED) and financially supported by the Japanese Ministry of Education, Culture, Sports, Science, and Technology. The dynamic test was carried out as the US-Japan collaboration and research funding was provided by U.S. National Science Foundation under award number CMMI-1000268 in support of this collaboration between U.S. and Japanese researchers. The authors express special thanks to their US collaborators; Prof. J. Moehle (UC Berkeley), Prof. R. Sauce (Lehigh U.), Prof. J. Wallace (UCLA), Prof. W. Ghannoum (U. of Texas), Mr. W. Keller and Ms. Z. Tuna.

## REFERENCES

Architectural Institute of Japan (2004), Guidelines for Structural Performance Evaluation of Earthquake Resistance Reinforced Concrete Building -Chapter 7 Performance assessment of walls, AIJ, pp. 195 - 231. (In Japanese)

Kono, S., Sakamoto, K., Sakashita, M., Mukai, T., Tani, M. and Fukuyama, H. (2012). Effects of boundary columns on the seismic behavior of cantilever structural walls, 15th World Conference on Earthquake Engineering. (Submitted)

HMME, (2012). Kuraves-Actis User's Manual, Ver. 1.50, Hozen Maintenance & Management Engineering Co. Ltd.

Nagae T., Tahara K, et al, (2011a). Large Scale Shaking Table Tests on a Four-Story RC Building, AIJ Structures Journal, Vol.76 , pp. 1961-1962. (In Japanese)

Nagae T. et al., (2011b). Design and Instrumentation of the 2010 E-Defense Four-Story Reinforced Concrete and Post-Tensioned Concrete Buildings, PEER 2011/104.

Nagae T. et al., (2012). Test results of Four-Story Reinforced Concrete and Post-Tensioned Concrete Buildings: The 2010 E-Defense Shaking Table Test, 15th World Conference on Earthquake Engineering. (Submitted)

Sakamoto K. et al, (2012). Experimental Study on Effect of Shear Reinforcement Ratio of Boundary Columns on Flexural Behavior of Structural Walls, Summaries of technical papers of Annual Meeting Architectural Institute of Japan. C-2, Structures IV. (Submitted, In Japanese)